Stress and Strain Patterns of 1-Piece and 2-Piece Implant Systems in Bone: A 3-Dimensional Finite Element Analysis

Zeev Ormianer, DMD,* Arial Ben Amar, DMD,† Mariusz Duda, DDS,‡ Sharon Marku-Cohen, DMD,§ and Israel Lewinstein, DMD, PhD‖

Statement of Problem: *The transition from implant to abutment is solid in 1-piece (1P) and broken in 2-piece (2P) implant designs. This difference may affect occlusal load distribution and marginal bone response.*

Purpose: *To determine whether 1P and 2P implants with equivalent geometries exhibited stresses and strains differently under applied loading conditions.*

Materials and Methods: *Design software simulated 1P and 2P implants restored with metal copings and embedded in 3 cylindrical bone block models that varied in dimensions, density, and percentage of bone-to-implant contact. Three-dimensional, finite element analysis simulated occlusal loading. Experiments evaluated stresses and strains relative to implant design and (1) periimplant bone thickness, (2) cortical bone thickness, (3) magnitude and direction of occlusal loading, and (4) % bone-to-implant contact.*

Results: *Implants with equivalent dimensions exhibited comparable stresses and strains in all experimental conditions. Implant diameter and periimplant bone thickness influenced stress levels. Only small-diameter (3.0 mm) 1P implants in low-density bone exhibited stress levels that might adversely affect marginal bone stability.*

Conclusions: *Implant diameter and periimplant bone thickness influenced load distribution in bone, but the type of implant-abutment transition had no significant effect. Small-diameter 1P implants should be limited to dense bone to minimize stress concentrations. (Implant Dent 2012;21:1–00)*

Key Words: 1-piece, 2-piece, dental implant, finite element analysis, bone

One-piece dental implants consist of implant and abutment sections manufactured together as a single unit. They were first introduced in the 1940s, and subsequently manufactured in a variety of designs and materials over 4 decades of clinical use.[1,2] After publication of seminal 10-year implant study of Brånemark et al[3] in 1977, 2-piece (2P) implants rapidly eclipsed the use of most 1-piece (1P) designs and continued to gain acceptance by mainstream dentistry through the 1990s. Growing patient acceptance of dental implants resulted in increased demands for shorter treatment time and improved aesthetics. In response, some clinicians began to advocate nonsubmerged placement of 2P implants, and others[4–9] subsequently experimented with immediate or early provisional loading. Although immediate and early loading studies were preliminary and short term, reports of generally favorable outcomes[4–9] helped to renew clinical interest in 1P implant designs for immediate provisionalization. The underlying rationale was that a 1P implant that replicated the overall geometry of a 2P implant system, but which eliminated potential abutment rotation,[10] screw loosening,[10] and bacterial colonization along the submucosal implant-abutment interfacial microgap,[11,12] might theoretically offer some clinical benefits over 2P implant systems.

The few published prospective studies[13–16] on 1P implants, however, have been short term and incapable of either substantiating or refuting this theory. Some clinicians feel that these concerns are not important with modern 2P implant systems that have stable implant-abutment connections, and that limited vertical access, difficulty in achieving optimal angulation, and the necessity of intraoral abutment preparations may limit the use of 1P designs. Other clinicians have also raised concerns that 1P designs may have a high potential for bone loss[15] and implant failure.[16]

Stress distribution in bone is a direct function of implant design. Stud-

*Lecturer, Department of Oral Rehabilitation, The Maurice and Gabriela Goldschleger School of Dental Medicine, University of Tel Aviv, Tel Aviv, Israel.
†Associate Professor, Head, Department of Oral Rehabilitation, The Maurice and Gabriela Goldschleger School of Dental Medicine, University of Tel Aviv, Tel Aviv, Israel.
‡Private Practice, Silesia—Med Oral Medicine Clinic, Katowice, Poland.
§Clinical Instructor, Department of Oral Rehabilitation, The Maurice and Gabriela Goldschleger School of Dental Medicine, University of Tel Aviv, Tel Aviv, Israel.
‖Senior Lecturer, Coordinator Department of Oral Rehabilitation, The Maurice and Gabriela Goldschleger School of Dental Medicine, University of Tel Aviv, Tel Aviv, Israel.

Reprint requests and correspondence to: Zeev Ormianer, DMD, Department of Oral Rehabilitation, the Maurice and Gabriela Goldschleger School of Dental Medicine, University of Tel Aviv, Tel Aviv, Israel, Phone: +972-3-6124224, Fax: +972-3-6124226, E-mail: drzeev@ormianer.com

ISSN 1056-6163/12/02101-001
Implant Dentistry
Volume 21 • Number 1

DOI: 10.1097/ID.0b013e31823fce22

Table 1. Bone Model Characteristics for FEA Analysis

	Bone Dimensions		Bone Character					
			Cortical		Trabecular		Homogenous	
Bone Model	Vertical Thickness (mm)	Horizontal Thickness* (mm)	Vertical Thickness (mm)	Elastic Modulus (GPa)	Vertical Thickness (mm)	Elastic Modulus (GPa)	Vertical Thickness (mm)	Elastic Modulus (GPa)
A	20	Various	—	—	—	—	20	3.5
B†	20	2	3	15	17	1.5	—	—
C‡	20	2	1	15	19	1.5	—	—

* Uniform periimplant bone thickness.

† Generally representative of D1 or D2 bone.[28]

‡ Generally representative of D2 or D3 bone.[28]

ies[17–20] using 3-dimensional (3D) finite element analysis (FEA) documented major variations in the abilities of different implant designs to resist and distribute vertical and lateral occlusal loads in bone. In FEA studies, microstrain ($\mu\epsilon$) is widely used as a method of measuring the load applied to bone as percent the tissue deformation. Frost[21] hypothesized that specific microstrain levels (thresholds) in bone tissue trigger biologic mechanisms that cause bone to either atrophy ($<$200 $\mu\epsilon$), maintain a balanced steady state (200–2500 $\mu\epsilon$), hypertrophy (2500–4000 $\mu\epsilon$), or suffer pathological overload ($>$4000 $\mu\epsilon$) that may result in bone resorption. Similar thresholds for pathological overload with secondary bone resorption have been reported by Sugiura et al[22] ($\approx$3600 $\mu\epsilon$ or 50 MPa).

Although contemporary 1- and 2P implant systems may have a similar gross external geometries, internal variations may result in very different patterns of load distribution. For example, it is currently unknown whether the interfacial break between the implant and abutment of 2P systems may enhance or reduce stress concentrations in the crestal bone region compared with 1P implant systems, which have a solid transition between the components.

This study reports on a 3D FEA study that compared load distribution patterns of simulated 1P and 2P implants with different diameters in various bone models. The null hypothesis of this study was that there would be no significant difference in load distribution between 1P and 2P dental implants under conditions of simulated loading. An alternate hypothesis was that 1P implants would exhibit higher stress concentrations than 2P implants in the crestal bone region, but that their resulting strain values would still fall within normal limits of 200 to 4000 $\mu\epsilon$[21] for crestal bone maintenance.

MATERIALS AND METHODS

Engineering design software (SolidWorks Professional 2006; SolidWorks Corp, Concord, MA) and 3D FEA code (ANSYS Workbench 11.0; ANSYS Inc., Canonsburg, PA) were used in a personal computer (XPS 210 Desktop; Dell, Round Rock, TX) with Microsoft Windows XP Professional (Microsoft Corp, Redmond, WA) software to create all digital study models. Each model consisted of either a simulated 1P (Zimmer 1-piece Implant; Zimmer Dental Inc., Carlsbad, CA) or 2P (Tapered Screw-Vent Implant and Hex-Lock Abutment; Zimmer Dental Inc.) implants embedded in 1 of 3 cylindrical bone blocks that differed in characteristics and uniform periimplant thicknesses (t) (Table 1). Implant components were modeled with an elastic modulus of 110 GPa and a Poisson's ratio of 0.34 GPa, which are consistent with titanium alloy,[23] and were positioned in accordance with the manufacturer's instructions for placement. Bone-to-implant contact (BIC) formed an interfacial bond between the modeled implants and bone blocks, but the percentage of BIC varied according to the experiment. A simulated titanium alloy coping was attached to each abutment to ensure the uniform transfer of applied load.

The finite element models consist of 4-node tetrahedron elements (consistent element size of 0.5 mm [0.020 in] for all assemblies); which total number of elements varied depending on the implant assembly size.

For the boundary conditions, the outer surface of the bone block was modeled as a fixed, and all of interfaces between components (ie, abutment, screw) were modeled as bonded except the interface between implant and abutment that was modeled as a sliding contact. Top portion of a 1P implant (outside of the bone) is still called abutment in this study though the implant and abutment are 1 piece.

To simulate occlusal loading, 222 N of occlusal force was applied to the implant model at a 30-degree angle (θ = 30 degrees) with a 1.5 mm buccolingual offset from the vertical axis of the implant. The selected occlusal force represented a slightly higher-than-median value within the range of 140[24] to 286.7 N,[25] which are mean maximum clenching force values documented in the incisor regions of healthy patients. Offset loading at a 30-degree angle was performed in an attempt to approximate normal occlusal patterns during mastication. Before the study, a preliminary experiment evaluated these prescribed boundary and load conditions in the lateral, premolar, and molar locations. The study consisted of 4 experiments that applied the same prescribed boundary and load conditions to simulated sites in the adult maxillary lateral incisor

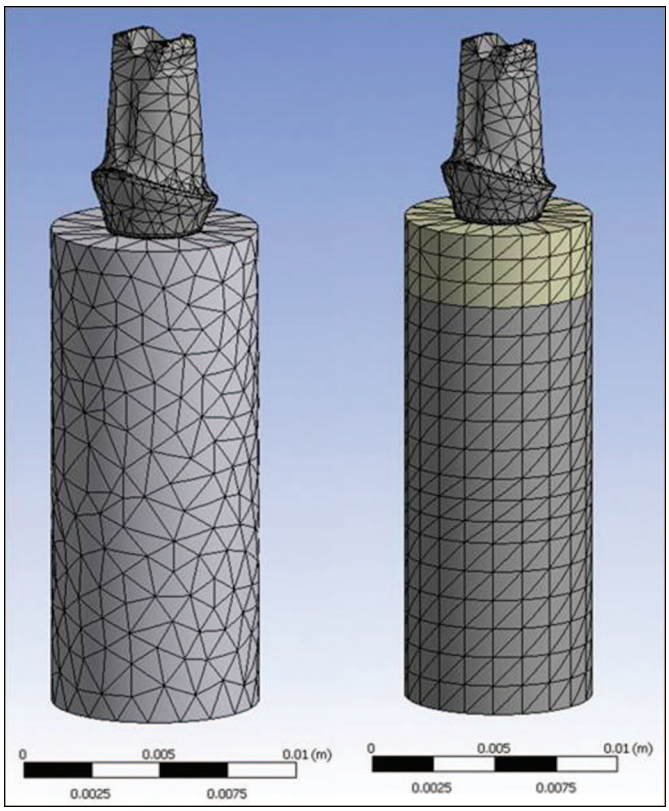

Fig. 1. Typical finite element analysis (FEA) model and meshes simulating a 1-piece implant embedded in bone with a homogenous structure (left) or defined cortical and cancellous layers (right).

region. This location represented the area of greatest aesthetic need because of its visual prominence and having the second-highest documented frequency of tooth loss[26] in the aesthetic zone. The 4 experiments evaluated the influences of implant design (1P or 2P) and diameter (3.0, 3.7, 4.1, 4.7, or 6.0 mm) on bone stress levels relative to 1 or more secondary variables.

Experiment 1 investigated the influence of periimplant bone thickness on stress levels in homogenous bone (Fig. 1). This experiment evaluated the findings of a prospective, multicenter clinical study[27] conducted by the US government on approximately 3000 implants. The study[27] measured the distance from the inner walls of newly prepared implant osteotomies to the outer surfaces of the residual buccal plates, and then correlated residual facial plate thicknesses to future facial bone loss and implant failure. Below the critical threshold of 2 mm facial bone thickness, facial plate resorption and implant failure rates increased.[27] When facial plate thickness was ≥2 mm, however, implant survival rates increased and some evidence of marginal bone gain was noted.[27] In this study, bone model A (Table 1)[28] was used and osseointegration was assumed to be complete (BIC = 100%). The isotropic, homogeneous elastic modulus of the bone model was based on documented[29,30] modula of 15 GPa for cortical bone (E_1) and 1.5 GPa for trabecular bone (E_2). Calculations of average elastic modulus utilized volume fractions of cortical bone (ν_1 = 15%) and trabecular cancellous bone (ν_2 = 85%) where ν_1, ν_2, E_1, and E_2 are volume fractions and elastic modulus of cortical and cancellous bone, respectively:

$$E = \upsilon_1 E_1 + \upsilon_2 E_2 \qquad (1)$$

A 2-time decay model was used to describe the FEA analysis data presented in Eq. (2) where C_1 and C_2 (MPa) are constants dependent on the implant assembly size and platform, t (mm) is the bone thickness surrounding the implant in mm, and τ_1 and τ_2 (mm) are decay constants:

$$\sigma(t) = C_1 \exp(-t/\tau_1) + C_2 \exp(-t/\tau_2) \qquad (2)$$

Experiment 2 investigated the influence of cortical bone vertical thickness. To simulate 2 different cortical bone thicknesses, the first and second segments of this experiment used bone models B and C (Table 1), respectively (Fig. 1). In both segments, osseointegration was assumed to be complete (BIC = 100%). In experiment 3, the influence of occlusal load magnitude and direction served as the secondary experimental variable. Bone model B (Table 1) was used, and osseointegration was assumed to be complete (BIC = 100%). Vertical compressive loading at a 0-degree angle (θ = 0 degrees) from the long axis of the implant model was also applied as part of the stress distribution analysis. The linear elastic model used in this study was expected to cause a linear increase in the maximum stress in the bone.

Experiment 4 investigated how the percentages of BIC (% BIC) influenced stress levels in bone model B (Table 1). BIC was 100% in the cervical and apical regions of the implant models, but ranged from 8% to 100% in the thread regions to approximately <100% osseointegration that really occurs *in vivo*, regardless of implant design.[31] This phenomenon of osseointegration is attributable, in part, to the fact that bone contains numerous marrow spaces that are not mineralized.[32]

RESULTS

Implant design, load (magnitude and direction), boundary conditions, and the quality, mechanical properties, and cortical thickness of bone all influenced bone stress levels in this study. Maximum bone stress levels for both 1P and 2P models in the preliminary experiment were below the yield stress of bone (180 MPa), regardless of placement region (incisor, premolar, and molar). Nearly all recorded stresses and strains in this study were <55 MPa and 3690 $\mu\epsilon$, respectively, for both 1P and 2P implants, regardless of loading conditions or bone

types. These values were less than the critical thresholds of stresses for bone resorption (60 MPa) and microstrain values for bone resorption (4000 $\mu\epsilon$).

In experiment 1, all maximum bone stress levels were 40 MPa or lower in 2-mm thick periimplant bone (Table 2). As periimplant bone thickness decreased to 1 mm, the standard diameter (3.7 mm) 1P design exhibited significantly higher stress distributions (42 MPa) than the 2P design (37 MPa) in the same diameter (Table 2). This difference diminished and stress distribution levels relatively converged between the 2 standard diameter designs as bone thickness increased to 2 mm or more (Table 2). In contrast, there was no difference in stress distribution between wide diameter (4.7 mm) 1P and 2P designs, regardless of periimplant bone thickness (Table 2).

Bone stress levels increased as periimplant bone thickness decreased for all implant designs and diameters (Table 2). For example, maximum bone stress levels for a 2P implant, 3.7 mm in diameter, ranged from 26 to 37 MPa as periimplant bone decreased from 2.5 to 1.0 mm, respectively (Table 2). In contrast, increasing implant diameter reduced bone stress levels despite a corresponding reduction in periimplant bone thickness. For example, a 1P implant, 3.0 mm in diameter with 2.0 mm of periimplant bone thickness, generated 40 MPa of maximum bone stress levels (Table 2). By increasing the implant diameter to 3.7 or 4.7 mm, periimplant bone thickness decreased to 1.5 and 1.0 mm, respectively, with corresponding reductions in maximum bone stress levels of 34 and 24 MPa (Table 2). Based on 2-time decay models, the rate of change in bone stress levels because of bone thickness was independent of the implant design or diameter (Table 2). The elevated stress levels generated by 1P implants, 3.0 mm in diameter, in periimplant bone <2-mm thick, may adversely affect crestal bone maintenance (Table 2).

In experiment 2, 1P and 2P designs in bone models B (Tables 1 and 3) and C (Tables 1 and 4) exhibited the highest stress contour bands in the crestal bone region, but stresses progressively diminished deeper within the bone. Implants in matching lengths and diameters demonstrated no significant differences in crestal bone stress concentrations, regardless of implant design. Although data showed that 1P and 2P models exhibited a 6 MPa difference in maximum von-Mises stress in 2-mm thick bone for both 3.7- and

Table 2. Influence of Implant Design, Diameter, and Periimplant Bone Thickness on Maximum Bone Stress Levels (MPa) in Bone Model A*

Periimplant Bone Thickness (*t*) (mm)	Maximum Bone Stress Levels (MPa)						
	1-Piece Implants by Diameter†			2-Piece Implants by Diameter†			
	3.0 mm	3.7 mm	4.7 mm	3.7 mm	4.1 mm	4.7 mm	6.0 mm
1.0‡	53	42	24	37	32	24	17
1.5	45	34	20	31	26	20	14
2.0	40	30	18	28	24	18	13
2.5	38	28	16	26	22	16	12
3.0	36	26	16	25	21	16	11
3.5	36	26	15	25	21	15	11
4.1	35	25	15	24	21	15	11
4.5	35	25	15	24	21	15	11
5.0	35	25	15	24	21	15	11

* FEA analysis using 222 N of load applied at a 30-degee angle and a 1.5 mm offset.

† Note that increasing implant diameter decreases periimplant bone thickness.

‡ Not recommended for actual clinical applications.

Table 3. Maximum Stress and Strain Values by Implant Design and Diameter in Bone Model B*

Implant Diameter (mm)	1P Implants		2P Implants		Difference (1P vs. 2P)	
	Stress (Max.) (MPa)	Microstrain (Max) ($\mu\epsilon$)	Stress (Max) (MPa)	Microstrain (Max) ($\mu\epsilon$)	Stress (Max) (MPa)	Microstrain (Max) ($\mu\epsilon$)
3.0	54	3637	—	—	—	—
3.7	47	3143	41	2750	6 (1P > 2P)	393 (1P > 2P)
4.1	—	—	37	2436	—	—
4.7	30	1980	24	1800	6 (1P > 2P)	180 (1P > 2P)
6.0	—	—	22	1656	—	—

* Refer Table 1.

1P indicates 1-piece; 2P, 2-piece.

Table 4. Maximum Stress and Strain Values by Implant Design and Diameter in Bone Model C*

Implant Diameter (mm)	1P Implants		2P Implants		Difference (1P vs. 2P)	
	Stress (Max.) (MPa)	Microstrain (Max.) ($\mu\epsilon$)	Stress (Max.) (MPa)	Microstrain (Max.) ($\mu\epsilon$)	Stress (Max.) (MPa)	Microstrain (Max) ($\mu\epsilon$)
3.0	77	5438	—	—	—	—
3.7	53	3633	55	3690	2 (2P > 1P)	57 (2P > 1P)
4.1	—	—	52	3483	—	—
4.7	41	2704	41	2750	None (1P = 2P)	46 (2P > 1P)
6.0	—	—	36	2542	—	—

* Refer Table 1.

1P indicates 1-piece; 2P, 2-piece.

Table 5. Maximum Stress and Strain Values by Implant Design and Diameter at 0-Degree Angle Load Vector in Bone Model B*

	1P Implants		2P Implants		Difference (1P vs. 2P)	
Implant Diameter (mm)	Stress (Max.) (MPa)	Microstrain (Max.) ($\mu\epsilon$)	Stress (Max.) (MPa)	Microstrain (Max.) ($\mu\epsilon$)	Stress (Max.) (MPa)	Microstrain (Max.) ($\mu\epsilon$)
3.0	29	1929	—	—	—	—
3.7	27	1781	24	1590	3 (1P > 2P)	191 (1P > 2P)
4.1	—	—	20	1401	—	—
4.7	16	1576	16	1561	None (1P = 2P)	15 $\mu\epsilon$ (1P > 2P)
6.0	—	—	13	1296	—	—

* Refer Table 1.

1P indicates 1-piece; 2P, 2-piece.

4.7-mm diameter implants (Table 3), maximum stresses still fell significantly below the critical threshold of 180 MPa associated with stress-related bone resorption. Errors in 3D modeling, meshing inconsistency between FEA models, and minor simulation errors caused this small difference. Apart from these minor factors, bone stress concentrations between simulated 1P and 2P implants in matching lengths and diameters exhibited no significant differences.

Vertical and lateral load stresses also decreased in inverse proportion to an increase in implant diameter, regardless of implant design. All stresses and strains observed under the prescribed boundary and load conditions were below approximately 54 MPa and 3637 $\mu\epsilon$, respectively, in bone model B (Table 3), and 55 MPa and 3690 $\mu\epsilon$, respectively, in bone model C (Table 4). The 1 exception to the latter finding, however, was exhibited by the 3.0-mm diameter 1P implant (smallest implant diameter in the study) placed into bone model C, which had minimal (1 mm) cortical bone thickness (Tables 1 and 4). In this model, stress values were higher than the bone yield point, which amounted to pathological overloading. This was the worst outcome in Experiment 2.

In experiment 3, all stresses and strains observed under the boundary and load conditions for 1P and 2P implants subjected to 0-degree angle occlusal load vector were <29 MPa and 1929 $\mu\epsilon$, respectively, for all implants diameters. These results do not account for the nonlinear response of bone. Comparison of 0- and 30-degree angle load directions indicated that off-axis loading generated significantly higher stress levels in bone than axial loading (Tables 5 and 6). For 1P and 2P implants subjected to 30-degree angle, occlusal load vector were higher up to 47 MPa and 2750 $\mu\epsilon$, respectively. Data suggest that those stresses will increase proportionately to the distance of off-axis loading. Increasing bone quality equates with a greater ability to withstand higher occlusal load magnitudes without failure. Cortical bone has higher stiffness values than the trabecular cancellous bone. Although bone stress values increased in cortical bone compared with cancellous bone, the mechanical properties of cortical bone were better able to bear higher stresses than cancellous bone. In that way, higher density bone will allow for better stabilization of the implant assembly as compared with lower density bone.

In experiment 4, up to approximately 50% BIC did not affect maximum bone stress values, but stress levels began rising as the % BIC decreased to <50%. The reduced % BIC slightly increased local stresses around the implant threads. Highest stress contour bands were located in the crestal bone region, but progressively decreased deeper within the trabecular bone. For most evaluations, stress levels within trabecular bone were less than 5 MPa under the prescribed boundary conditions based on typical von-Mises stress contours.

DISCUSSION

Vertical and transverse occlusal loads produce stress gradients in implant systems and surrounding bone. The manner in which an implant system transfers the resulting axial and off-axial forces and bending moments to the supporting bone directly affects its survival and long-term crestal bone maintenance. Many different variables can influence load distribution, such as implant geometry and dimensions, material properties, surface characteristics, the % BIC, bone volume and properties, prosthesis type, and load vector angles relative to the implant axis. FEA has been widely used since the late 1970s to convert these complex biomechanical relationships into more simplistic mesh elements, analyze them at a functional level, and then reassemble the data to predict the patterns and effects of stress on dental implants and the surrounding tissues. This task requires the formulation of many assumptions and theoretical constructs, all of which entail some inherent margin of error.

In this study, each FEA study model consisted of a simulated implant embedded in a block of bone measuring 1 to 5 mm in thickness around the implant. Although FEA implant studies commonly use this type of model, the design inherently skews generated stress values because of the limited bone volume. An implant placed into a rectangular bone block with 1 to 5 mm of bone thickness on the simulated buccal and lingual aspects of the implant, but significantly greater bone volume on its simulated mesial and distal aspects, may more accurately simulate stress dispersal in bone comparable with that of an actual implant placed into the alveolar process.

Although the cylindrical bone block model may have somewhat ele-

Table 6. Maximum Stress and Strain Values by Implant Diameter and Design in Bone Model B*: Comparison of Load Direction (0-Degree Angle vs. 30-Degree Angle)

Implant Diameter (mm)	Unit	Maximum Stress and Microstrain Values					
		1P Implants			2P Implants		
		30 degrees	0 degrees	Difference (%)	30 degrees	0 degrees	Difference (%)
3.0	Stress (MPa)	54	29	(−) 46	—	—	—
	Microstrain ($\mu\epsilon$)	3637	1929	(−) 47	—	—	—
3.7	Stress (MPa)	47	27	(−) 43	41	24	(−) 42
	Microstrain ($\mu\epsilon$)	3143	1781	(−) 43	2750	1590	(−) 42
4.1	Stress (MPa)	—	—	—	37	20	(−) 46
	Microstrain ($\mu\epsilon$)	—	—	—	2436	1401	(−) 43
4.7	Stress (MPa)	30	16	(−) 47	24	16	(−) 33
	Microstrain ($\mu\epsilon$)	1980	1576	(−) 20	1800	1561	(−) 33
6.0	Stress (MPa)	—	—	—	22	13	(−) 41
	Microstrain ($\mu\epsilon$)	—	—	—	1656	1296	(−) 22

* Refer Table 1.

1P indicates 1-piece; 2P, 2-piece.

vated stress values in this study, the use of a rectangular bone block would probably not have altered the observed relationships between study variables. In other words, reducing simulated lingual and buccal plate thickness of an implant placed in a rectangular bone block model would still result in elevated bone stress values, but those stress values would probably not be as high as stresses generated in a cylindrical bone block model with less volume to absorb stresses.

Other discrepancies in this study included the assumed 100% bonding the between the implant and abutment in the 2P model, and the assumed 100% BIC in some experiments. In reality, manufacturing tolerances would not allow a 100% bond between all interlocking implant-and-abutment geometrical surfaces in this design, but the friction-fit interface that is achievable would probably render the difference between the simulated model and the actual components negligible in terms of stress generation. In a similar manner, performing the experiments in question with <100% BIC might affect recorded stress levels somewhat, but the relationships between the variables would probably not be significantly different. These preliminary findings on the differences in load distribution between 1P and 2P implant designs require further investigation.

CONCLUSIONS

Within limitations of this study, 1P and 2P implant models of equivalent endosseous geometries and diameters did not exhibit significantly different stress distributions in bone. According to these analyses, wider implant diameters, thicker periimplant bone, thicker cortical bone, reduced load magnitudes, and smaller load vector angles to the long axis of the implant can help to reduce bone stress levels.

DISCLOSURE

The authors claim to have received the numeric modules of implant from Zimmer.

ACKNOWLEDGMENTS

The authors thank Mike Werner, Zimmer Dental, Carlsbad, CA, for his technical support.

REFERENCES

1. Ring ME. Pause for a moment in dental history. A thousand years of dental implants: A definitive history-part 2. *Compend Contin Educ Dent*. 1988;14:1132–1142.

2. Schroeder A, van der Zypen E, Stich H, et al. The reactions of bone, connective tissue, and epithelium to endosteal implants with titanium-sprayed surfaces. *J Maxillofac Surg*. 1981;9:15–25.

3. Brånemark PI, Hansson BO, Adell R, et al. Osseointegrated implant in the treatment of the edentulous jaw. Experience from a 10-year period. *Scand J Plast Reconstr Surg Suppl*. 1977;16:1–132.

4. Jokstad A, Carr AB. What is the effect on outcomes of time-to-loading of a fixed or removable prosthesis placed in implant(s)? *Int J Oral Maxillofac Implants*. 2007;22:19–48.

5. Avila G, Galindo P, Rios H, et al. Immediate implant loading: Current status from available literature. *Implant Dent*. 2007;16:235–245.

6. Del Fabbro M, Testori T, Francetti L, et al. Systematic review of survival rates for immediately loaded dental implants. *Int J Periodontics Restorative Dent*. 2006;26:249–263.

7. Ioannidoue E, Doufexi A. Does loading time affect implant survival? A meta-analysis of 1,266 implants. *J Periodontol*. 2005;76:1252–1258.

8. Attard NJ, Zarb GA. Immediate and early implant loading protocols: A literature review of clinical studies. *J Prosthet Dent*. 2005;94:242–258.

9. Gapski R, Wang HL, Mascarenhas P, et al. Critical review of immediate implant loading. *Clin Oral Impl Res*. 2003;14:515–527.

10. Vogel RE, Davliakos JP. Spline implant prospective multicenter study: Interim report on prosthetic screw stability in partially edentulous patients. *J Esthet Restor Dent*. 2002;14:225–237.

11. Broggini N, McManus LM, Hermann JS, et al. Persistent acute inflammation at the implant-abutment interface. *J Dent Res*. 2003;82:232–237.

12. Jones AA, Cochran DL. Consequences of implant design. *Dent Clin N Am*. 2006;50:339–360.

13. Parel SM, Schow SR. Early clinical experience with a new one-piece implant

system in single tooth sites. *J Oral Maxillofac Surg*. 2005;63(suppl 2):2–10.

14. Finne K, Rompen E, Tolijanic J. Clinical evaluation of a prospective multicenter study on one-piece implants. Part 1: Marginal bone level evaluation after 1 year of follow-up. *Int J Oral Maxillofac Implants*. 2007;22:226–234.

15. Ostman PO, Hellman M, Albrektsson T, et al. Direct loading of NobelDirect and Nobel Perfect one-piece implants: A 1-year prospective clinical and radiographic study. *Clin Oral Impl Res*. 2007;18: 409–418.

16. Albrektsson T, Gottlow J, Meirelles L, et al. Survival of NobelDirect implants: An analysis of 550 consecutively placed implants at 18 different clinical centers. *Clin Implant Dent Relat Res*. 2007;9:65–70.

17. Rieger MR, Mayberry M, Brose MO. Finite element analysis of six endosseous implants. *J Prosthet Dent*. 1990;63: 671–676.

18. Huang HL, Chang CH, Hsu JT, et al. Comparison of implant body designs and threaded designs of dental implants: A 3-dimensional finite element analysis. *Int J Oral Maxillofac Implants*. 2007;22:551–562.

19. Bozkaya D, Muftu S, Muftu A. Evaluation of load transfer characteristics of five different implants in compact bone at different load levels by finite element analysis. *J Prosthet Dent*. 2004;92:523–530.

20. Lin S, Shi S, LeGeros RZ, et al. Three-dimensional finite element analyses of four designs of a high-strength silicon nitride implant. *Implant Dent*. 2000;9:53–60.

21. Frost HM. Bone's mechanostat: A 2003 update. *Anat Rec A Discov Mol Cell Evol Biol*. 2003;275:1081–1101.

22. Sugiura T, Horiuchi K, Sugimura M, et al. Evaluation of threshold stress for bone resorption around screw based on in vivo strain measurement of miniplate. *J Musculoskelet Neuronal Interact*. 2000; 1:165–170.

23. Chun HJ, Shin HS, Han CH, et al. Influence of implant abutment type on stress distribution in bone under various loading conditions using finite element analysis. *Int J Oral Maxillofac Implants*. 2006;21:195–202.

24. Hellsing G. On the regulation of interincisor bite force in man. *J Oral Rehabil*. 1980;7:403–411.

25. Tortopidis D, Lyons MF, Baxendale RH, et al. The variability of bite fore measurement between sessions, in different positions with the dental arch. *J Oral Rehabil*. 1998;25:681–686.

26. Marcus SE, Drury TF, Brown LJ, et al. Tooth retention and tooth loss in the permanent dentition of adults: United States, 1988–1991. *J Dent Res*. 1996;75: 684–695.

27. Spray JR, Black CG, Morris HF, et al. The influence of bone thickness on facial marginal bone response: Stage 1 placement through stage 2 uncovering. *Ann Periodontol*. 2000;5:119–128.

28. Misch CE. Density of bone: Effect on treatment plans, surgical approach, healing, and progressive bone loading. *J Oral Implantol*. 1990;6:23–31.

29. van Rossen IP, Braak LH, de Putter C, et al. Stress-absorbing elements in dental implants. *J Prosthet Dent*. 1990;64: 198–205.

30. Geng JP, Tan KBC, Liu GR. Application of finite element analysis in implant dentistry: A review of the literature. *J Prosthet Dent*. 2001;85:585–598.

31. Todisco M, Trisi P. Histomorphometric evaluation of six dental implant surfaces after early loading in augmented human sinuses. *J Oral Implantol*. 2006;32: 153–166.

32. Schupbach P, Hurzeler M, Grunder U. Implant-tissue interfaces following treatment of peri-implantitis using guided tissue regeneration. A light and electron microscopic study. *Clin Oral Impl Res*. 1994;5:55–65.